

**NMR backbone assignment and dynamics of Profilin from Heimdallarchaeota**

**Syed Razaul Haq<sup>1</sup>, Sabeen Survery<sup>1</sup>, Fredrik Hurtig<sup>1</sup>, Ann-Christin Lindås<sup>1\*</sup> and Celestine N. Chi<sup>2\*</sup>.**

<sup>1</sup>Department of Molecular Bioscience, Wenner-Gren Institute, Stockholm University, Svante Arrhenius v. 20C, SE-10691 Stockholm, Sweden

<sup>2</sup>Department of Medical Biochemistry and Microbiology, Uppsala University, BMC Box 582, SE-75123 Uppsala, Sweden.

\*Corresponding authors: ann.christin.lindas@su.se, chi.celestine@imbim.uu.se

Keywords: profilin, Archaea, chemical shifts, eukaryogenesis, actin, NMR spectroscopy

## Abstract

The origin of the eukaryotic cell is an unsettled scientific question. The Asgard superphylum has emerged as a compelling target for studying eukaryogenesis due to the previously unseen diversity of eukaryotic signature proteins. However, our knowledge about these proteins is still relegated to metagenomic data and very little is known about their structural properties. Additionally, it is still unclear if these proteins are functionally homologous to their eukaryotic counterparts. Here, we expressed, purified and structurally characterized profilin from Heimdallarchaeota in the Asgard superphylum. The structural analysis shows that while this profilin possess similar secondary structural elements as eukaryotic profilin, it contains additional secondary structural elements that could be critical for its function and an indication of divergent evolution.

### 1    **Biological context**

2    The origin of the eukaryotic cell remains an unsettled scientific question and several hypotheses have been put  
3    forward to explain the complex evolutionary history of the eukaryotic cell<sup>1 2 3 4</sup>. The Woese hypothesis proposes  
4    three domains of life - Archaea, Bacteria and Eukaryota, with independent evolutionary trajectories<sup>5</sup>. The eocyte  
5    hypothesis suggests the existence of only two domains - bacteria and archaea, and that eukaryotes emerged from  
6    the symbiotic relationship of an unknown archaeal host with an alphaproteobacterium<sup>6</sup>. Recently, environmental  
7    metagenomic sampling led to the discovery of the Asgard superphylum. Comparative genomic analysis of Asgard  
8    archaea and eukaryotes appears to support the eocyte hypothesis<sup>7</sup>. The genomes of Asgardarchaea are enriched  
9    with proteins previously considered eukaryote-specific, so called eukaryotic signature proteins (ESPs), and  
10   phylogenetic analysis placed the Asgardarchaea in a monophyletic group with eukaryotes<sup>8</sup>.

11        Actin plays a crucial part of the eukaryotic cytoskeleton and is essential to many processes, including  
12   cellular motility, cell division, endocytosis, intracellular cargo transport, amongst many other<sup>9</sup>. Because of the  
13   central role actin plays in the eukaryotic cell, the sequence of actin remains highly conserved among eukaryotes.  
14   While actin homologues are widespread throughout all domains of life, the dynamic actin cytoskeleton and the  
15   regulatory actin-binding proteins are a hallmark of eukaryotic life.

16        The Asgard genomes contain close actin homologues and several actin-binding proteins; including profilin,  
17   gelsolin, Arp2/3 complex subunit 4 and a large family of small GTPases that regulate the actin cytoskeleton in  
18   eukaryotes<sup>8</sup>. This posits the question; do these archaea possess an actin cytoskeleton with complex regulation  
19   analogous with the eukaryotic cytoskeleton? While metagenomic analysis has identified these proteins, their  
20   cellular function is still poorly understood. Laboratory culturing of these organisms is still in early development

which makes *in vivo* comparison with eukaryotic homologs difficult<sup>10</sup>. Currently, protein production in heterologous expression systems and reconstitution of the purified complexes *in vitro* represents one of the best approaches in characterizing their function. Profilin is expressed in most, if not all, eukaryotic cells and is one of the most important proteins in regulating actin cytoskeletal dynamics<sup>11</sup>. Eukaryotic profilin (eprofilin) is a small protein (approximately 14-19 kDa) which sequester monomeric G-actin from the cytoplasmic pool, thus controlling polymerization<sup>12</sup>. Despite significant divergence at the sequence level, the eprofilin tertiary structure is well-conserved and folds into 3D structures constituting 7 β-strands and 4 α-helices<sup>13</sup>. eprofilin promotes the elongation of actin filament assembly at the barbed end by acting as a nucleotide exchange factor, and by interacting with elongation factors such as Ena/Vasp, Formins, and Wasp<sup>14-16</sup>. These nucleation factors bind eprofilin through a polyproline motif at a domain physically separate from the actin binding-site. Moreover, eprofilin can also bind to phosphatidylinositol 4,5-bisphosphate (PIP<sub>2</sub>)<sup>17</sup> at the plasma membrane which results in a reduced affinity towards polyproline and actin<sup>17</sup>. eprofilin also competes with phospholipase C for PIP<sub>2</sub> binding which leads to interference with the PI3K/AKT signaling pathway<sup>18</sup>.

Recently, it has been shown that profilins encoded in several lineages of the Asgardarchaea not only share structural similarity with eukaryotic orthologues but are able to regulate the function of eukaryotic actin. This implies that profilin from Asgardarchaea have the potential of complex regulation of the hypothetical actin cytoskeleton as well<sup>19</sup>. In contrast to human profilin I, a previous study showed that the Asgard profilins (Loki 1 and 2, Thor, Odin and Heimdall) did not show polyproline binding. This led the authors to suggest that Asgard profilins do not bind polyproline, and that polyproline directed actin assembly is a later addition in eukaryotic evolution<sup>19</sup>. However, PIP<sub>2</sub> was shown to modulate the affinity of Asgard profilin towards rabbit actin in a functional assay<sup>19</sup>. Nevertheless, some of the Asgard genomes are incomplete and the structural and functional relationships of representative profilins from different Asgard lineages are still poorly understood. It might therefore be too early to assume that Asgard profilins do not bind polyproline. In addition, the crystal structures of various profilins combined with functional data do not only reveal structural similarity between Asgard profilins, but also highlights some subtle differences at the species level<sup>19</sup>. Within the Asgard superphylum, the Heimdallarchaeota appears to currently be the closest relative of eukaryotes<sup>7</sup>. Here we present the NMR backbone assignment and dynamics of the Heimdallarchaeota profilin (heimProfilin) as a first step towards characterizing it structurally. These NMR amino acid specific assignments and dynamics provide for the first time an atomic snapshot of heimProfilin as well as providing further evidence for the idea that the Asgard encoded proteins possess similar structural elements and are likely to perform similar roles as those in eukaryotes.

## 51 **Methods and experiments**

### 52 **Protein expression and purification**

53 Heimdallarchaeota profilin (GenBank: OLS22855.1) was cloned into the pSUMO-YHRC vector, kindly provided by  
54 Claes Andréasson (Addgene Plasmid #54336; RRID: Addgene\_54336) with an N-terminal 6xHistidine-tag and a  
55 SUMO-tag (cleavable with Ulp1 protease). The vector was transformed and expressed in *E. coli* Rosetta DE3 cells.  
56 Initially, the cells were grown in 2x TY media at 37 °C until the optical density of the culture was 0.8 at 600 nm.  
57 Cells were then harvested by centrifugation at 4000 x g for 15 minutes at 4 °C and washed twice with M9 medium.

58 The cells were then transferred into M9 media supplemented with 1g/L  $^{15}\text{N}$ -ammonium chloride and 1g/L  $^{13}\text{C}$ -  
59 glucose and grown for 1 hour at 30 °C. Protein expression was induced by 0.5 mM IPTG. For Deuterium ( $^2\text{H}$ )  
60 labelling, the M9 medium was prepared with 100% or 50%  $\text{D}_2\text{O}$  and cells were grown overnight at 30 °C. Post-  
61 induction, the cells were harvested by centrifugation and resuspended in the binding buffer (50 mM Tris-HCl pH  
62 7.5, 0.3 M NaCl, 1 mM TCEP, 10 mM imidazole, 10% glycerol). The cells were then lysed by sonication and the cell  
63 lysate was clarified by centrifugation at 25,000 x g for 45 min at 4 °C and finally filtered through a 0.2  $\mu\text{m}$  syringe  
64 filter (Sarstedt). The supernatant was loaded onto a His GraviTrap column (1ml, GE healthcare) and the bound  
65 protein was eluted with binding buffer containing 250 mM imidazole. The protein was incubated with Ulp1  
66 protease overnight at 4 °C to cleave the SUMO-tag including the Histidine-tag. The protein was desalted using a  
67 PD10 column (GE Healthcare) and loaded onto a His GraviTrap column again to remove the tag and the Ulp1  
68 protease. The protein was concentrated using a 10,000 NMWL cutoff centrifugal filter (Merck Millipore) and  
69 further purified on a Superdex 75 10/300 GL (GE Healthcare) size exclusion column, equilibrated with 25 mM Tris-  
70 HCl, 50 mM NaCl, 5% Glycerol, 1 mM TCEP at pH 7.5. Protein concentration was determined using the molar  
71 absorption coefficient at 280 nm (29450/M/cm).

72

### 73 **NMR Spectroscopy**

74 Double labeled  $^{15}\text{N}$ ,  $^{13}\text{C}$ , or triple labeled  $^{15}\text{N}$ ,  $^{13}\text{C}$ ,  $^2\text{H}$  were prepared to a concentration of 20 mg/ml in 25 mM Tris-  
75 HCl, 50 mM NaCl, 5% Glycerol, 1 mM TCEP at pH 7.5 and thereafter supplemented with 3%  $\text{D}_2\text{O}$  and 0.03% sodium  
76 azide. The NMR assignment experiments were performed at 308K on a triple-resonance Bruker 900, 700 or 600  
77 MHz spectrometers equipped with a cryogenic probe. NMR relaxation experiments were performed on a 600 MHz  
78 spectrometer at 298 K. Backbone sequence-specific assignments were carried out using the following experiments  
79 2D  $^1\text{H}$ - $^{15}\text{N}$ -TROSY, 3D TROSY-HNCACCB, 3D TROSY-HNCA, 3D TROSY-CO) CACB and 3D TROSY-HN(CO)CA. For side-  
80 chain assignments, 2D  $^1\text{H}$ - $^{13}\text{C}$  CT-HSQC, 3D HBHA(CO)NH and 3D HCCH-TOCSY spectra were utilized. For assignment  
81 and fold verification 3D NOESY as well as  $^3J_{\text{HHH}\alpha}$  for secondary structure verification were measured. For Backbone  
82  $R_1$ ,  $R_2$  rates and hetero-nuclear NOES were determined in an interleaved manner with the experiments from the  
83 Bruker pulse program library. For  $R_1$  and  $R_2$  rates, the relaxation delay was sampled for 9 and 8 delay-durations  
84 which were pseudo-randomized, respectively ( $R_1$ : 20, 60, 100, 200, 400, 600, 800 and 1000 ms and  $R_2$ : 16, 33, 67,  
85 136, 170, 203, 237 and 271 ms). The relaxation delay time was up to 1.5 s for  $R_1$  and 1 s for  $R_2$ . The  $[^1\text{H}]^{15}\text{N}$ -hetNOE  
86 experiment and a reference spectra were recorded with a total 2 s  $^1\text{H}$  saturation time for the NOE experiment and  
87 the same recovery time for the reference experiment. The order parameter  $S^2$  and the internal correlation time  
88 were calculated with the program dynamic center. The rotational diffusion tensor was estimated from the ratio of  
89 the relaxation rates ( $R_1$  and  $R_2$ ). TALOS and CYANA were employed to predict secondary structure, using  $^1\text{H}^N$ ,  $^{15}\text{N}$ ,  
90 and  $^{13}\text{C}^\alpha$  chemical shifts. All other data were processed with topspin and analyzed using CCPNMR<sup>20</sup> and CYANA<sup>21</sup>.

### 91 **Assignment and data deposition**

92 The expressed and purified heimProfilin corresponds to the full length as was generated from metagenomics data<sup>8</sup>.  
93 It consists of 148 amino acids which was purified with a cleavable tag that leaves no additional N-terminal amino  
94 acids (see methods). This profilin possesses a 20-amino acid extension compared with the previously characterized

95 eprofilins or those from Loki I and II and Odin. We obtained up to 88% of all backbone and up to 80% of all side-  
96 chain assignments. 135 of the 148 non-proline amide residues were assigned in the  $^1\text{H}$ - $^{15}\text{N}$  TROSY (Fig. 1). The  
97 following amides were not possible to assign: M1, K2, D3, I6, K11, K14, I19, S25, E27, N62, S85 and N89. The  
98 missing amides could be due to motional broadening or fast solvent exchange. We obtained 92% of the  $\text{C}_\alpha$  and  $\text{C}_\beta$   
99 resonance assignments.  $\text{H}_\beta$  and  $\text{H}_\alpha$  proton shifts were completed to 97% and 96%, respectively. These assignments  
100 were further verified by  $^{15}\text{N}/^{13}\text{C}$  3D NOESY spectra. Backbone and side-chain chemical shifts assignments have  
101 been deposited to the Biological Magnetic Resonance Data Bank (BMRB) with the Accession Number 50190.

102 **Secondary structure analysis**

103 The structures of eukaryotic and Asgard profilin from Loki (1 and 2) and Odin have been determined by X-ray  
104 crystallography<sup>19</sup>. However, no structural information is available from the heimProfilin which appears to be the  
105 closest relative to the eukaryotes. With the completed assignments, it was now possible to analyze the secondary  
106 structure characteristics of this profilin to see if it adopts similar secondary structural elements. Analysis of  
107 sequential and medium range NOEs revealed stretches of dNN, dNN(i, i+2), d $\alpha\beta$ (i, i+3), d $\alpha\text{N}$ (i, i+3). Residues 29–  
108 33, 64–68, 124–127 and 125–144 continual revealed d $\alpha\text{N}$  (i, i+4) NOEs, indicating the presence of helices in this  
109 region. This is supported by the  $^3J_{\text{HNN}\alpha}$  coupling constants for these residues which display small values typical of  
110 alpha helices (Fig. 2).  $^{13}\text{C}_\alpha$  and  $\text{C}_\beta$  shifts are frequently used to predict secondary structure propensities.  $\text{C}_\alpha$  shifts  
111 generally tend to shift upfield in a beta-sheet and extended strands relative to the random coil values. In alpha  
112 helices, these  $\text{C}_\alpha$  shifts tend to shift downfield<sup>22</sup>. For  $\text{C}_\beta$  values the opposite is true, they shift downfield for beta-  
113 sheets and extended strands and upfield for alpha helices. The  $\text{C}_\alpha$  and  $\text{C}_\beta$  values relative to random coil values are  
114 shown in figure 2. Examination of these plots indicates clear helical regions covering residues 29–34, 64–68, 124–  
115 127 and 135–144. The helical region between residues 64–68 has not been observed in previous profilin structures.  
116 The region of beta strands also agrees with NOEs values and slightly increased  $^3J_{\text{HNN}\alpha}$  values. This analysis indicates  
117 that the overall secondary structural elements are preserved from archaea to eukaryotes albeit with some slight  
118 differences in their lengths. In addition, we observed an additional helix between residues 64–68 which was not  
119 present in the previously determined profilin structures. This might be important for modulating profilin-actin  
120 interaction and other physiological roles.

121 **Backbone dynamics**

122  $R_1$  and  $R_2$  rates in addition to  $[^1\text{H}]\text{-}^{15}\text{N}$  hetNOE are frequently used to estimate the flexibility of proteins<sup>23</sup>. Deviation  
123 of  $R_1$  and  $R_2$  rates for  $[^1\text{H}]\text{-}^{15}\text{N}$  moieties from the average value often indicate a change in motional property.  $R_1$   
124 values that are larger than the average indicates the presence of flexibility in the ps-ns time range. On the other  
125 hand,  $R_2$  rates with higher values than the average indicates regions of slow conformational exchange in the  $\mu\text{s}$ -ms  
126 time scale.  $[^1\text{H}]\text{-}^{15}\text{N}$  hetNOE with negative or near zero values indicate regions of high flexibility with motions faster  
127 than approximately 1 ns. We measured and plotted the longitudinal  $R_1$  and transverse  $R_2$  rates as well the  $[^1\text{H}]\text{-}^{15}\text{N}$   
128 hetNOE versus amino acids sequence (Fig. 3). Overall, the results from these values indicate a highly rigid protein  
129 between residues 25–148 (Fig. 2). However, N-terminal residues 1–24 show a high degree of flexibility, which is

130 reflected in the very low [<sup>1</sup>H]-<sup>15</sup>N hetNOE values (Fig. 2). We also back calculate order parameter  $S^2$  and internal  
131 correlation time  $\tau_e$ . A plot of the calculated order parameter  $S^2$  and internal correlation time  $\tau_e$  is shown in figure  
132 3d. As shown in the plot, only the N-terminal 1-24 amino acids show some degree of flexibility with very low order  
133 parameter and high degree of internal motion. A few residues along the protein sequence indicate some degree of  
134 flexibility. We determined the correlation time  $\tau_c$  of 11.3 ns. This value is slightly higher for a protein of this size  
135 indicating probably due to the extended N-terminal loop not completely structured.

136

### 137 **Conclusions**

138 In this study, we have determined the NMR backbone and dynamic data of a profilin from Heimdallarchaeota in  
139 the Asgard superphylum. Our secondary structure analysis indicates that this profilin possess similar structural  
140 elements to eukaryotic homologues, all beit at varied lengths. Our data also indicates that the heimProfilin appears  
141 rigid apart from N-terminal residues 1-24 which are not present in previously characterized eukaryotic profilins.  
142 We observed an additional helix between residue 64-68 which lies in the interface of the actin binding site when  
143 compared to eukaryotic profilin, and likely plays a role in modulating actin polymerization.

### **Acknowledgments:**

### 144 **Declarations**

**Funding:** This work was supported by Wenner-Gren Stiftelsen Fellow's Grants, Ake Wiberg, Magnus Bergvall and O.E Edla Johannsson foundation grants to CC, Swedish Research Council Grant 621-2013-4685 for FH and Wellcome Trust Grant 203276/F/16/Z for SRH, SS and FH. This study made use of the NMR Uppsala infrastructure, which is funded by the Department of Chemistry - BMC and the Disciplinary Domain of Medicine and Pharmacy.

**Conflicts of interest/Competing interests:** the authors declare no conflict of interest. **Ethics approval:** not applicable. **Consent to participate:** not applicable. **Consent for publication:** all authors read an approved the manuscript. **Availability of data and material:** all data and material are available and can be obtain from the authors

### 145 **Figure legends**

146 **Figure 1** | 1H-15N TROSY correlation spectrum of Heimdallarchaeota profilin. All <sup>1</sup>H-<sup>15</sup>N pairs that were assigned in  
147 this study. Side-chains of Glutamine and Asparagine are not assigned or shown.

**Figure 2** | Secondary structure characterization of Heimdallarchaeota profilin. (a) Sequence-specific <sup>13</sup>C <sub>$\alpha$</sub>  secondary chemical shifts ( $\delta\Delta^{13}\text{C}_{\alpha}$ ) along the amino acid sequence of heimProfilin. (b) <sup>3</sup>J<sub>HNH $\alpha$</sub>  couplings plotted as a function of amino acid sequence. (c) TALOS secondary structure prediction based on <sup>1</sup>H, <sup>15</sup>N and <sup>13</sup>C <sub>$\alpha$</sub>  shifts plotted as function of amino acid sequence. All three suggest the presence of helical and extended strands in similar regions. The presence of helices between residues 29-34, 64-68, 124-127 and 135-144 are clearly visible. <sup>3</sup>J<sub>HNH $\alpha$</sub>  couplings are generally lower for helices (2-4 Hz) and higher for beta strands and extended regions (2-8 Hz). Very few <sup>3</sup>J<sub>HNH $\alpha$</sub>

couplings were obtained for residues 1-20. However, the  $^{13}\text{C}_\alpha$  shifts and the TALOS prediction clearly shows that this region is extended.

**Figure 3** | Dynamic characterization of the backbone based on  $[^1\text{H}]-[^{15}\text{N}]$ . (a) Longitudinal  $^{15}\text{N}$   $R_1$  relaxation rates plotted as a function of amino acid sequence. (b) Transverse  $^{15}\text{N}$   $R_2$  relaxation rates versus the amino acid sequence. (c)  $[^1\text{H}]-[^{15}\text{N}]$ -hetero-nuclear NOE data (hetNOE) along the amino acid sequence. (d) calculated  $S^2$  order parameter (left axis) and internal motion  $\tau\text{e}$  (right axis) plotted as a function of the amino acid sequence. All parameters indicate a very rigid molecule structure from the N-terminal 20 amino acids which show some degree of ps-ns motion based on the elevated  $R_1$ , lower hetNOE and lower  $S^2$  order parameter.

Figure 1

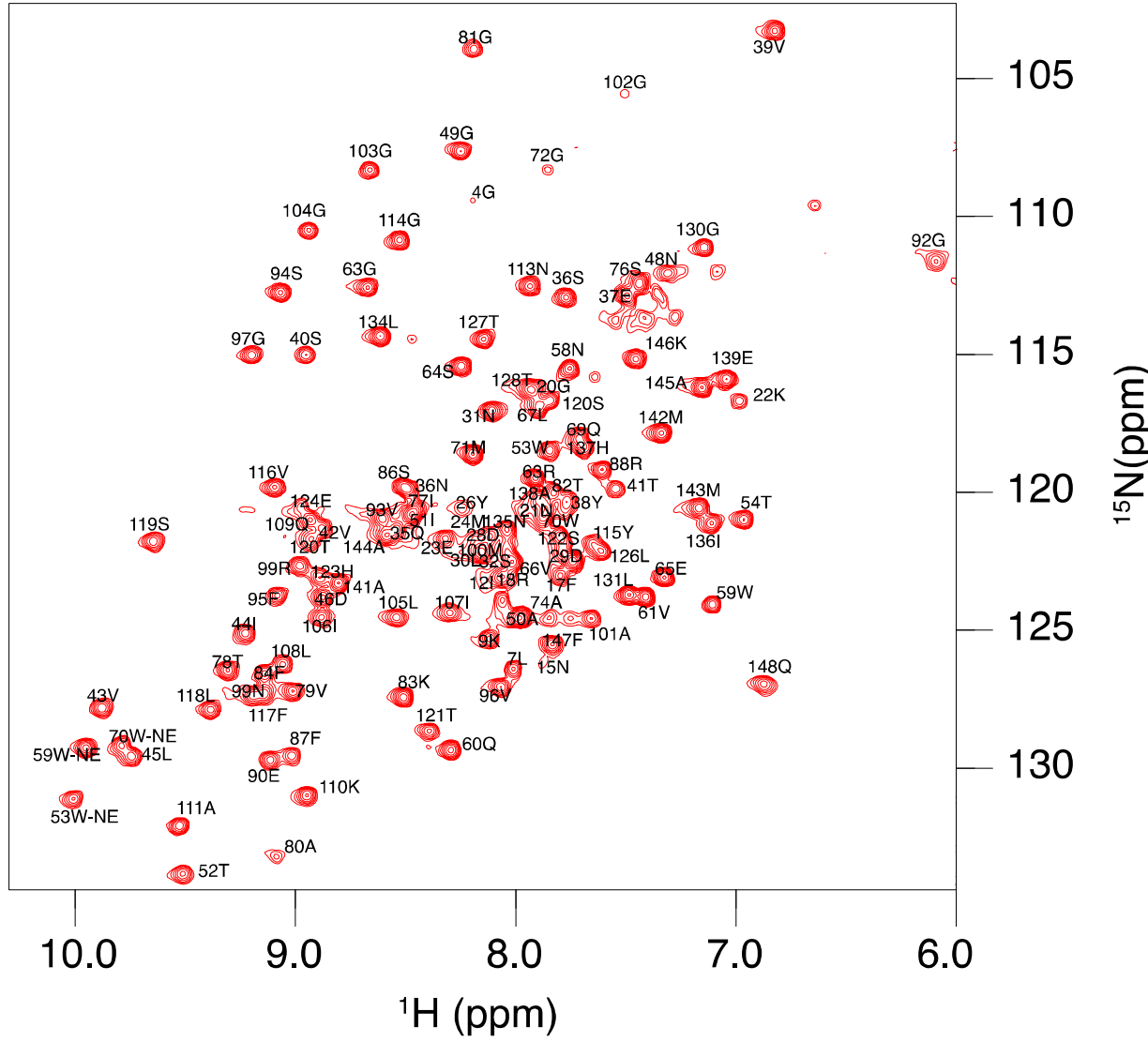


Figure 2

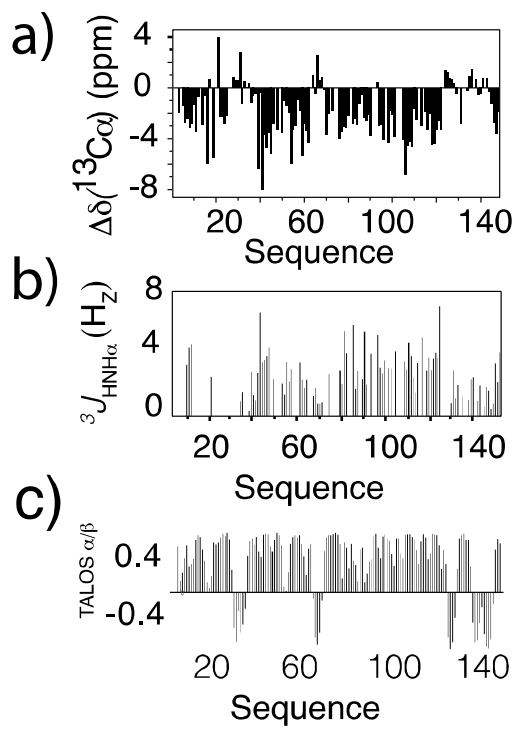
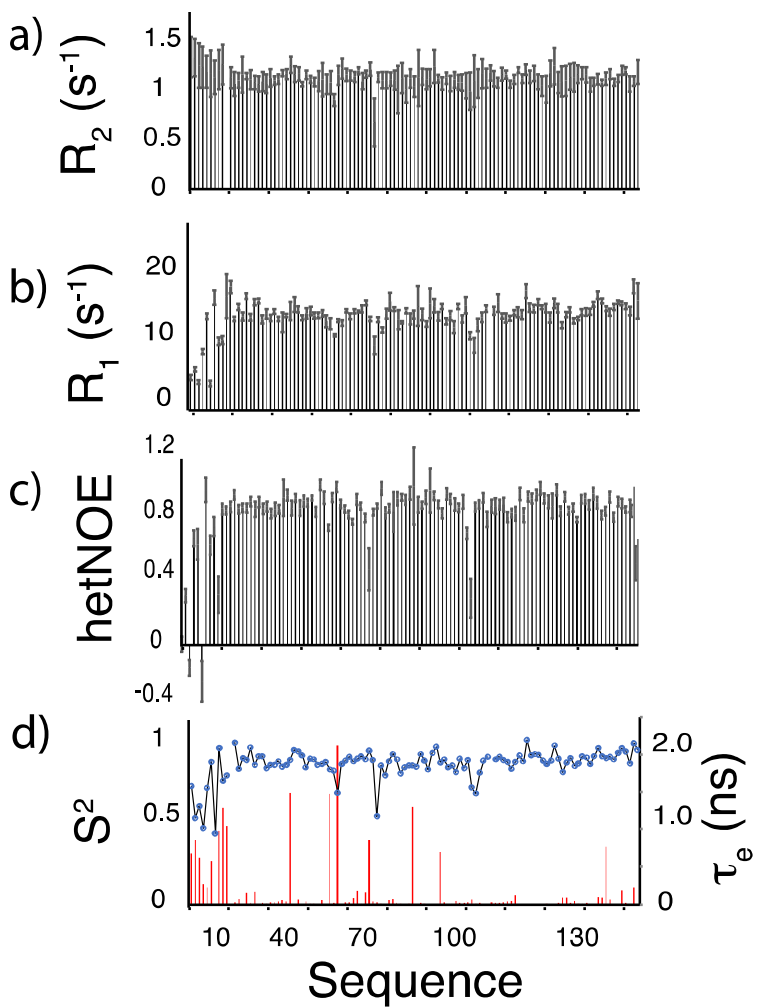


Figure 3



#### References:

148 1. Koonin, E.V. Origin of eukaryotes from within archaea, archaeal eukaryome and bursts of gene gain:  
 149 eukaryogenesis just made easier? *Philos Trans R Soc Lond B Biol Sci* **370**, 20140333 (2015).  
 150 2. Lopez-Garcia, P. & Moreira, D. Open Questions on the Origin of Eukaryotes. *Trends Ecol Evol* **30**, 697-  
 151 708 (2015).  
 152 3. Da Cunha, V., Gaia, M., Gadelle, D., Nasir, A. & Forterre, P. Lokiarchaea are close relatives of  
 153 Euryarchaeota, not bridging the gap between prokaryotes and eukaryotes. *PLoS Genet* **13**, e1006810  
 154 (2017).  
 155 4. Spang, A. et al. Asgard archaea are the closest prokaryotic relatives of eukaryotes. *PLoS Genet* **14**,  
 156 e1007080 (2018).  
 157 5. Woese, C.R., Kandler, O. & Wheelis, M.L. Towards a natural system of organisms: proposal for the  
 158 domains Archaea, Bacteria, and Eucarya. *Proc Natl Acad Sci U S A* **87**, 4576-9 (1990).  
 159 6. Lake, J.A., Henderson, E., Oakes, M. & Clark, M.W. Eocytes: a new ribosome structure indicates a  
 160 kingdom with a close relationship to eukaryotes. *Proc Natl Acad Sci U S A* **81**, 3786-90 (1984).  
 161 7. Spang, A. et al. Complex archaea that bridge the gap between prokaryotes and eukaryotes. *Nature* **521**,  
 162 173-179 (2015).  
 163 8. Zaremba-Niedzwiedzka, K. et al. Asgard archaea illuminate the origin of eukaryotic cellular complexity.  
 164 *Nature* **541**, 353-358 (2017).  
 165 9. Pollard, T.D. Actin and Actin-Binding Proteins. *Cold Spring Harb Perspect Biol* **8**(2016).  
 166 10. Imachi, H. et al. Isolation of an archaeon at the prokaryote-eukaryote interface. *Nature* **577**, 519-525  
 167 (2020).  
 168 11. Schluter, K., Jockusch, B.M. & Rothkegel, M. Profilins as regulators of actin dynamics. *Biochim Biophys  
 169 Acta* **1359**, 97-109 (1997).  
 170 12. Birbach, A. Profilin, a multi-modal regulator of neuronal plasticity. *Bioessays* **30**, 994-1002 (2008).  
 171 13. Schutt, C.E., Myslik, J.C., Rozycki, M.D., Goonesekere, N.C. & Lindberg, U. The structure of crystalline  
 172 profilin-beta-actin. *Nature* **365**, 810-6 (1993).

173 14. Reinhard, M. et al. The proline-rich focal adhesion and microfilament protein VASP is a ligand for  
174 profilins. *EMBO J* **14**, 1583-9 (1995).

175 15. Kursula, P. et al. High-resolution structural analysis of mammalian profilin 2a complex formation with two  
176 physiological ligands: the formin homology 1 domain of mDia1 and the proline-rich domain of VASP. *J  
177 Mol Biol* **375**, 270-90 (2008).

178 16. Goldschmidt-Clermont, P.J. et al. The control of actin nucleotide exchange by thymosin beta 4 and profilin.  
179 A potential regulatory mechanism for actin polymerization in cells. *Mol Biol Cell* **3**, 1015-24 (1992).

180 17. Lambrechts, A. et al. The mammalian profilin isoforms display complementary affinities for PIP2 and  
181 proline-rich sequences. *EMBO J* **16**, 484-94 (1997).

182 18. Sathish, K. et al. Phosphorylation of profilin regulates its interaction with actin and poly (L-proline). *Cell  
183 Signal* **16**, 589-96 (2004).

184 19. Akil, C. & Robinson, R.C. Genomes of Asgard archaea encode profilins that regulate actin. *Nature* **562**,  
185 439-443 (2018).

186 20. Vranken, W.F. et al. The CCPN data model for NMR spectroscopy: development of a software pipeline.  
187 *Proteins* **59**, 687-96 (2005).

188 21. Guntert, P., Mumenthaler, C. & Wuthrich, K. Torsion angle dynamics for NMR structure calculation with  
189 the new program DYANA. *J Mol Biol* **273**, 283-98 (1997).

190 22. Berjanskii, M.V. & Wishart, D.S. A simple method to predict protein flexibility using secondary chemical  
191 shifts. *J Am Chem Soc* **127**, 14970-1 (2005).

192 23. Palmer, A.G. Enzyme Dynamics from NMR Spectroscopy. *Accounts of Chemical Research* **48**, 457-465  
193 (2015).